Dynamic Energy Router

ENERGY MANAGEMENT IN ELECTRICAL SYSTEMS FED BY MULTIPLE SOURCES

ANTONIO SÁNCHEZ-SQUELLA, ROMEO ORTEGA, ROBERT GRIÑÓ, and SHANE MALO

PHOTO BY DENNIS BERNSTEIN

In this article we consider the objective of efficient transfer of electric energy between subsystems, where each subsystem can generate, store, or consume energy. An application example is a multidomain system consisting of a fuel-cell-based generating unit, batteries, supercapacitors, and electric motors or generators; this topology is used in some electric cars. Depending on the operation regime, energy must be transferred between the various units, which we refer to as multiports, according to some energy-management policy. To ensure energy exchange, the interconnection of the storage and load devices is performed by using power converters. These subsystems are electronically switched circuits capable of adapting the port voltage or current magnitudes to a desired value.

To achieve energy transfer between multiports, it is common practice to assume that the system operates in steady state and then translates the power demand (flow sense and magnitude) of the multiports into current or voltage references. These references are then tracked with control loops, usually proportional plus integral (PI). Since the various multiports have different time responses, it is often necessary to discriminate between quickly and slowly changing power-demand profiles. For instance, due to physical constraints, it is not desirable to demand quickly changing power profiles to a fuel-cell unit. Hence, the peak demands of the load are usually supplied by a bank of supercapacitors, whose time response is fast. To achieve this objective, a steady-state viewpoint is again adopted, and the current or voltage references to the multiports are passed through lowpass or highpass filters. For further details, see "Criteria for Current-Reference Selection."

The steady-state approach currently adopted in practice can only approximately achieve the desired objectives of energy transfer and slow-versus-fast discrimination of the power demand. In particular, during the transients or when fast dynamic response is required, the delivery of demanded power in response to current or voltage references and the time response action of the filters might be far from satisfactory.

In this article we present an energy router that dynamically controls energy flow. The router operational principle

Digital Object Identifier 10.1109/MCS.2010.938096

1066-033X/10/$26.00©2010IEEE

Criteria for Current-Reference Selection

The definition of the reference current $i_j^{\star}(t)$ described in the section "Power Electronic Implementation of the DSER" can complement additional constraints aimed at satisfying, for example, instantaneous reactive power specifications in electrical power applications. In addition, and to discriminate between quickly and slowly changing power demands, the current reference might be filtered with lowpass, highpass, or bandpass filters before being sent to the power converter controller.

Due to the slow dynamics of fuel cells, in combined implementation with other sources, the current reference of the fuel-cell port comes from the load current passed by a lowpass filter. As shown in Figure S1, the sum of the current references of ports 1 and 2 is the current reference of port 3. In this way, the fast response of the supercapacitor is used to supply high power demands. Furthermore, in this particular example, the voltage terminals of the three ports are considered to have the same value; otherwise, the current-reference shape is given by

$$i_1\frac{V_1}{V_3} + i_2\frac{V_2}{V_3} = i_3.$$

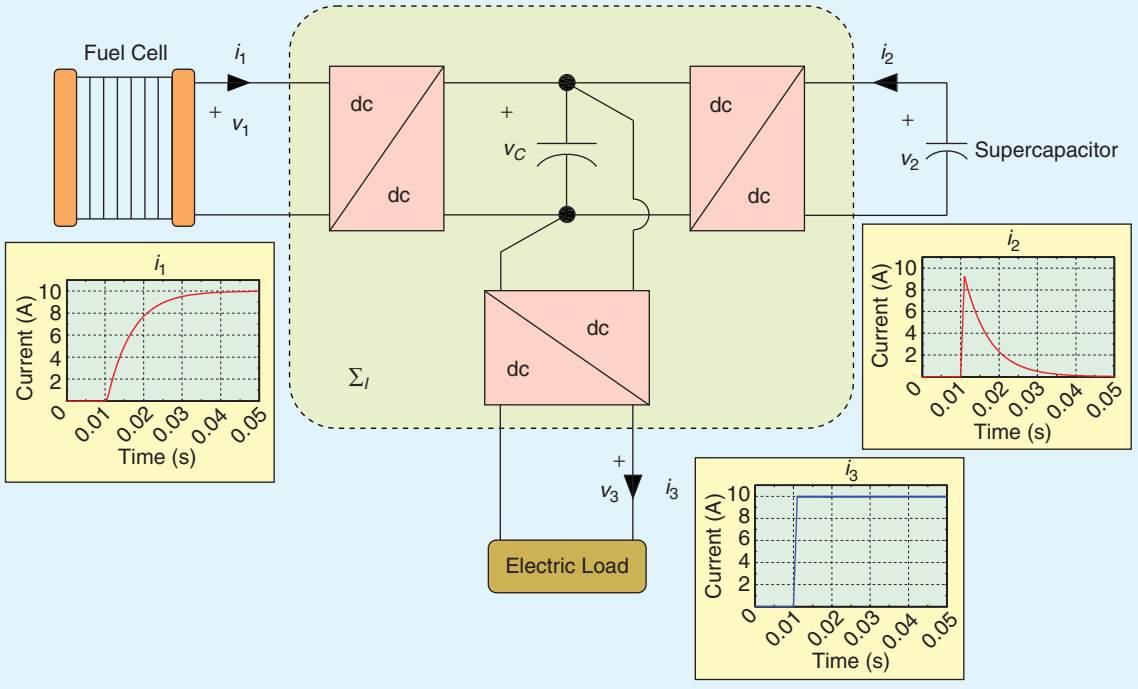

FIGURE S1 An example of current references in a multiport system with a fuel-cell source unit, a supercapacitor as a storage unit, and a generic electric load. In this example, the current load experiences a fast increment. Since the fuel cell cannot follow this quickly changing current demand, the supercapacitor supplies the current difference. To maintain the value of v_C, it is essential that the power delivered matches the power demand in applications using this kind of power converter. In this example the voltages v_1, v_2, and v_3 are considered equal, and the interconnection is lossless. Therefore, due to power balance, the addition of the supplied currents must agree with the load current.

presented in [1] and [2] discriminates between "good" and "bad" energy within the context of walking robots. A brief review of this device, which we call the Duindam-Stramigioli energy router (DSER), is given below from the perspective of electrical networks. The DSER embodies a nonlinear transformation that instantaneously transfers energy among multiports. The flow direction and rate of change of the energy transfer are regulated by means of a single scalar parameter. The goal of this article is to show that the DSER can be implemented by using standard power electronic converter topologies. Moreover, it is shown in [3] and [4] that nonlinear controllers can be used to determine the switching policy of the power converter. Therefore, the DSER can provide the basis for a physically viable device for high-performance energy-management applications. Simulation results for a two-subsystem example illustrate the performance of this approach.

This article is organized as follows. In the next section, the energy-management problem is formulated, a procedure used for its solution is reviewed, and DSER is

described. In the following section a power electronic implementation of DSER is presented. Illustrative results are given in the section "Simulation Results." The article ends with some concluding remarks.

The main objective of this article is to present the operational principles of the DSER and a power electronics implementation. We do not address technological considerations such as alternative circuit topologies or handling of the losses in the DSER. These topics, which are relevant to developers and designers of power electronics converters, are discussed in [5].

FORMULATION OF THE ENERGY-TRANSFER PROBLEM

It is assumed that the multiports denoted by Σ have as port variables the terminal voltages and currents, which we denote as $v(t), i(t) \in \mathbb{R}^m$, respectively; see Figure 1. It is also assumed that the multiports satisfy the energy-conservation law

$$\text{stored energy} = \text{supplied energy} - \text{dissipated energy}. \quad (1)$$

To formalize (1) the following assumptions are made.

i) The stored energy is represented by the nonnegative scalar function $\widetilde{H}\colon \mathbb{R}^n \to [0, \infty)$, whose argument $x \in \mathbb{R}^n$ is the state vector of the multiport. In an electrical circuit, x consists of electric charges in the capacitors and magnetic fluxes in the inductors.

ii) The supplied energy is given by the integral of the power delivered by or demanded from the external environment, that is,

$$H_S(t) = \int_0^t v^\top(s) i(s) ds. \quad (2)$$

iii) For $t \geq 0$ the dissipated energy is given by the integral of a nonnegative function representing power. For instance, the rate of energy flow through the resistive element R is given by $Ri_R^2(t)$, where $R > 0$ is the value of the resistor and $i_R(t)$ is the current flowing through the resistor. Therefore the dissipated energy is

$$d(t) = \int_0^t Ri_R^2(s) ds. \quad (3)$$

With this notation the energy-conservation law (1) becomes

$$H(t) - H(0) = \int_0^t v^\top(s) i(s) ds - d(t), \quad (4)$$

where $H(t) := \widetilde{H}(x(t))$. Since $d(t) \geq 0$, we have

$$H(t) - H(0) \leq \int_0^t v^\top(s) i(s) ds. \quad (5)$$

The inequality (5) implies that, at each instant of time, the increase of stored energy cannot exceed the external supplied energy (2).

Differentiating (4) and noting that $\dot{d}(t) = Ri_R^2(t) \geq 0$ for all t, we obtain

$$\dot{H}(t) \leq v^\top(t) i(t), \quad (6)$$

which means that the rate of increment of stored energy is less than or equal to the power delivered by or demanded from the system. To accomplish the energy exchange, the system we consider is composed of q multiport subsystems Σ_j, with energy functions $H_j(t)$ and port variables $(v_j(t), i_j(t))$, $j = 1, \ldots, q$, satisfying the power relation (6). These multiport subsystems are interconnected to exchange energy according to a specified energy-management policy.

The typical procedure for achieving energy transfer proceeds as follows [6]–[9]. Assume that at time $t \geq 0$ a demand $P_j^*(t)$ of power is requested from multiport Σ_j. Measuring the voltage $v_j(t)$, the power demand is then transformed into a current reference $i_j^*(t)$, solving the instantaneous power relation

$$P_j^*(t) = v_j^\top(t) i_j^*(t).$$

The terminal variables of the multiports are usually interconnected by power converters, which are circuits that apply the desired current or voltage profile to the multiport. In steady state, the desired energy-transfer objective is achieved asymptotically, thereby driving the current tracking error $i_j^*(t) - i_j(t)$ to zero. Toward this end, the switching policy of the converter is determined with a PI loop around the current error.

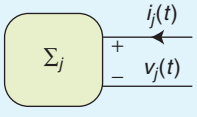

FIGURE 1 Representation of a subsystem, such as fuel cell or battery, as a multiport, denoted by Σ_j, with port variables $v_j(t)$ and $i_j(t)$. It is assumed that the multiport satisfies the energy-conservation law, which implies that the supplied energy is equal to the stored energy plus the dissipated energy. The studied system consists of q multiport systems Σ_j, with energy functions $H_j(t)$ and port variables $(v_j(t), i_j(t))$, $j = 1, \ldots, q$, satisfying the power relation (6).

THE DUINDAM-STRAMIGIOLI ENERGY ROUTER

Dynamic energy transfer is a time-varying energy rate according to the operational energy needs of the system. The operation of the DSER is briefly reviewed in this section; for further details see [2].

For simplicity, we first consider temporarily the case of two multiports. Moreover, we are interested in energy-management applications where the dissipated energy is

In this article we present an energy router that dynamically controls energy flow.

negligible, that is, $d_1(t), d_2(t) \approx 0$. Therefore, the power inequality (6) becomes

$$\dot{H}_1(t) = v_1^\top(t) i_1(t), \quad \dot{H}_2(t) = v_2^\top(t) i_2(t). \tag{7}$$

Assume that, at time $t \geq 0$, it is desired to instantaneously transfer energy from multiport Σ_2 to multiport Σ_1 without losses. Therefore, we require that

$$v_1^\top(t) i_1(t) + v_2^\top(t) i_2(t) = 0, \tag{8}$$

with

$$\dot{H}_1(t) > 0, \quad \dot{H}_2(t) < 0. \tag{9}$$

Equation (9) ensures that $H_1(t)$ decreases, while $H_2(t)$ increases, as desired.

To accomplish the energy transfer objective we couple the multiports through another multiport subsystem Σ_I, called the interconnection subsystem shown in Figure 2. To satisfy constraint (8), the device Σ_I must be lossless, that is, the total energy loss is zero; this condition is traditionally called *power-preserving*, which refers equivalently to the fact that the rate of energy loss is zero. The negative feedback interconnection, that is, $i_1 = v_2$, $i_2 = -v_1$, is a particular case of a lossless interconnection.

A lossless interconnection that satisfies (9) is the DSER, which is defined by

$$\Sigma_I = \begin{bmatrix} 0 & \alpha(t) v_1(t) v_2^\top(t) \\ -\alpha(t) v_2(t) v_1^\top(t) & 0 \end{bmatrix}. \tag{10}$$

The relation between the port variables is thus

$$\begin{bmatrix} i_1(t) \\ i_2(t) \end{bmatrix} = \begin{bmatrix} 0 & \alpha(t) v_1(t) v_2^\top(t) \\ -\alpha(t) v_2(t) v_1^\top(t) & 0 \end{bmatrix} \begin{bmatrix} v_1(t) \\ v_2(t) \end{bmatrix}, \tag{11}$$

where $\alpha(t) \in \mathbb{R}$ is a possibly time-varying designer-chosen parameter that, as shown below, controls the direction and rate of change of the energy flow.

Multiplying (11) on the left by the row vector $[v_1^\top(t) \quad v_2^\top(t)]$ yields (8). Hence, Σ_I is lossless. Furthermore, substituting the current expressions of (11) into (7) yields

$$\dot{H}_1(t) = \alpha(t) |v_1(t)|^2 |v_2(t)|^2,$$
$$\dot{H}_2(t) = -\alpha(t) |v_1(t)|^2 |v_2(t)|^2,$$

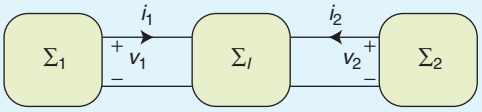

FIGURE 2 Interconnection subsystem, denoted by Σ_I. To couple multiports Σ_1 and Σ_2 satisfying the power-preservation restriction, the interconnection subsystem must be lossless. The power-preserving interconnection Σ_I controls the energy-flow magnitude and direction.

which shows that if $\alpha(t) > 0$, then (9) is satisfied. Note that the DSER ensures only that $H_1(t)$ is nonincreasing and $H_2(t)$ is nondecreasing. However, when the voltages are nonzero, which is the normal operating condition, the desired energy exchange occurs.

The energy direction can also be inverted, that is, if $\alpha(t) < 0$, then the energy flows from Σ_2 to Σ_1. Moreover, the energy transfer rate can also be regulated with a suitable selection of $\alpha(t)$. For instance, regulating the rate of change of $\alpha(t)$, the energy flow can be made faster or slower providing the ability to comply with restrictions on time responses of the multiports. These features of the DSER are illustrated in the section "Simulation Results."

The DSER defined by (11) is a current-tracking multiport. That is, given $v_1(t), v_2(t)$, (11) defines the desired values to be imposed on the multiport currents. A dual, voltage-tracking DSER can be defined as

$$\begin{bmatrix} v_1(t) \\ v_2(t) \end{bmatrix} = \begin{bmatrix} 0 & \alpha(t) i_1(t) i_2^\top(t) \\ -\alpha(t) i_2(t) i_1^\top(t) & 0 \end{bmatrix} \begin{bmatrix} i_1(t) \\ i_2(t) \end{bmatrix},$$

which yields

$$\dot{H}_1(t) = \alpha(t) |i_1(t)|^2 |i_2(t)|^2, \quad \dot{H}_2(t) = -\alpha(t) |i_1(t)|^2 |i_2(t)|^2.$$

The selection between current-tracking or voltage-tracking implementations of the DSER depends on technological considerations, which are discussed in "Power Electronics Considerations." In the current-tracking case $\alpha(t)$ controls the direction and rate of change of the energy flow. Therefore, $\alpha(t)$ must be selected by considering the energy-exchange needs and physical constraints on the system, for example, the maximum current or voltage tolerated by the system.

A more general form for the energy router is obtained by considering the generic interconnected system

The Duindam-Stramigioli energy router embodies a nonlinear transformation that instantaneously transfers energy among multiports.

$$\begin{bmatrix} i_1(t) \\ i_2(t) \end{bmatrix} = \begin{bmatrix} 0 & \beta(t) \\ -\beta(t) & 0 \end{bmatrix} \begin{bmatrix} v_1(t) \\ v_2(t) \end{bmatrix}, \tag{12}$$

where the matrix $\beta(t) \in \mathbb{R}^{m \times m}$ is chosen such that the power conditions (9) are satisfied. Multiplying both sides of (12) by $[v_1(t)^\top \quad v_2(t)^\top]$ yields

$$\begin{bmatrix} v_1^\top(t) i_1(t) \\ v_2^\top(t) i_2(t) \end{bmatrix} = \begin{bmatrix} v_1^\top(t)\, \beta(t) v_2(t) \\ -v_2^\top(t)\, \beta(t) v_1(t) \end{bmatrix}.$$

In the DSER, $\beta(t) = \alpha(t) v_1(t) v_2^\top(t)$, while alternative choices of this parameter are suitable for achieving the desired energy transfer, for example, the introduction of a saturation function in $\beta(t)$ is a technique for limiting the energy exchange between multiports. Therefore, a useful choice for energy management is

$$\beta(t) = \alpha(t) \phi_1(v_1(t)) \, (\phi_2(v_2(t)))^\top,$$

where $\phi_i : \mathbb{R}^m \to \mathbb{R}^m$ are first-third quadrant mappings, that is, ϕ_i satisfies $a^\top \phi_i(a) > 0$ for all $a \in \mathbb{R}^m$. By suitable selection of these functions, it is possible to modulate the contribution of each multiport to the overall power delivered.

In the development above, it is assumed that the dissipated energy is negligible. More precisely, the dissipated energy in the resistors is assumed to be smaller than the energy transferred between the multiports, which is the case in many energy-management scenarios. The correct performance of the DSER cannot be ensured when this is not the case.

POWER ELECTRONICS IMPLEMENTATION OF THE DSER

We now consider practical implementation to realize the energy transfer defined by (11). For simplicity, and without loss of generality, only scalar multiports are considered. Since no assumption is made regarding the nature of the port variable signals, the multiports may be alternating current (ac) or direct current (dc) systems. The selection of the port characteristics imposes additional technological constraints on the circuit topology, which are briefly discussed in the conclusions.

The switching circuit depicted in Figure 3 is a topology that can be used to implement the DSER. For further details about implementation, see "Power Electronics Considerations." Assuming that the switching frequency of the power converter is sufficiently fast and applying Kirchhoff's laws to this converter, the dynamics of the DSER are described by

$$L_1 \frac{di_1}{dt}(t) = -R_1 i_1(t) - v_C(t) u_1(t) + v_1(t), \tag{13}$$

$$L_2 \frac{di_2}{dt}(t) = -R_2 i_2(t) - v_C(t) u_2(t) + v_2(t), \tag{14}$$

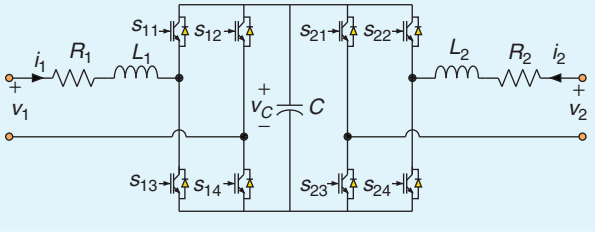

FIGURE 3 Static converter used to implement the energy router. The fundamental characteristic of this converter is its bidirectional energy exchange feature. The port variables, namely, voltages $(v_1(t), v_2(t))$ and currents $(i_1(t), i_2(t))$, are specified on both sides of the converter. Since this converter enables alternating voltage connection, the scheme is expandable to energy-exchange applications in ac systems.

Power Electronics Considerations

In (16) and (17), it is assumed that $v_C(t)$ is bounded away from zero and that the derivatives of the current references are known. It follows from physical considerations that, when the capacitance C is sufficiently large, $v_C(t)$ remains positive and bounded. Indeed, in this case a time-scale separation between the currents and the capacitor voltage is enforced. Consequently, in the limit the capacitor behaves as a constant-voltage source. Moreover, since high voltage implies fewer losses for a given power delivery and the power converters are normally voltage boosters, the voltage of the link capacitor must be kept positive and greater than v_1 and v_2 to ensure energy exchange [5]. In other words, the energy-storage device is customized for the power converter and vice versa. Furthermore, the chosen power electronic converter and the link energy-storage device define the tracking technique, that is, current or voltage tracking. For example, in the case of extracting energy from a current source, the voltage is modulated to regulate the energy exchange. Therefore, this current source system requires alternative power converters, switches, switching policy, and signal tracking.

$$C\dot{v}_C(t) = u_1(t)i_1(t) + u_2(t)i_2(t), \tag{15}$$

where $i_1(t)$, $i_2(t)$ are the inductor currents, $v_C(t)$ is the voltage in the capacitor, and $u_1(t), u_2(t) \in (0, 1)$ are the duty cycles of the switches, which represent the control signals. See [3] and [5] for additional details on modeling power converter devices. The remaining problem is now to design a control law that ensures that the currents track their desired references defined in (11), namely,

$$\begin{bmatrix} i_1^*(t) \\ i_2^*(t) \end{bmatrix} = \begin{bmatrix} \alpha(t)v_1(t)v_2^2(t) \\ -\alpha(t)v_2(t)v_1^2(t) \end{bmatrix},$$

where i_1^* and i_2^* are the desired port currents. The problem of controller design for power converter systems of the form described by (13)–(15) is considered in the power electronics and control literature [3]–[5]. To present the operational principles of the DSER, we consider the feedback linearization

$$u_1(t) = \frac{1}{v_C(t)}\left[v_1(t) - R_1 i_1(t) - L_1\frac{di_1}{dt}(t) + L_1\gamma\tilde{i}_1(t)\right], \tag{16}$$

$$u_2(t) = \frac{1}{v_C(t)}\left[v_2(t) - R_2 i_2(t) - L_2\frac{di_2}{dt}(t) + L_2\gamma\tilde{i}_2(t)\right], \tag{17}$$

where $\gamma > 0$ is a tuning parameter, and the tracking errors are defined by

$$\tilde{i}_1(t) = i_1(t) - i_1^*(t), \qquad \tilde{i}_2(t) = i_2(t) - i_2^*(t).$$

Replacing (16) and (17) in (13) and (14), respectively, yields

$$\dot{\tilde{i}}_1(t) = -\gamma\tilde{i}_1(t), \quad \dot{\tilde{i}}_2(t) = -\gamma\tilde{i}_2(t), \tag{18}$$

which implies that the current-tracking errors converge to zero exponentially fast, at a rate determined by γ, achieving the desired objective.

The derivatives of the reference currents used in (16) and (17) can be obtained using approximate differentiators. Alternative schemes that avoid differentiation can be derived from the results in [3] and [4].

SIMULATION RESULTS

Simulation results using Matlab are carried out to illustrate the performance of the DSER. The multiports Σ_1 and Σ_2 are taken as linear RC circuits, as shown in Figure 4. The energy functions of the multiports are

$$H_1(t) = \frac{C_1}{2}v_1^2(t), \qquad H_2(t) = \frac{C_2}{2}v_2^2(t).$$

Their dynamics are described by

$$C_1\dot{v}_1(t) = -i_1(t) - \frac{1}{R_C}v_1(t),$$

$$C_2\dot{v}_2(t) = -i_2(t) - \frac{1}{R_C}v_2(t).$$

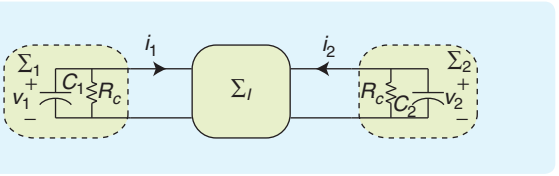

FIGURE 4 Interconnection of linear capacitors, chosen as subsystems. Each capacitor model contains a parallel resistor R_C, which in the simulations is not considered due to its high value. The capacitance of each capacitor is 250 F, which corresponds to a supercapacitor. This magnitude is related to the storage capability and voltage variation, and thus only slight variations of the voltages $v_1(t)$ and $v_2(t)$ are expected. Capacitances on the order of hundreds or thousands of μF are normally used for voltage regulation. On the other hand, capacitances on the order of hundreds of F are used for storage elements.

The parameters are chosen as $C_1 = 250$ F and $C_2 = 250$ F. The value of R_C is on the order of MΩ for capacitors used as energy-storage devices.

The control signals of the DSER, generated from (16) and (17), are the duty cycles of a pulse-width modulated (PWM) scheme operating at 15 kHz. The controller gain is set to $\gamma = 1000$. The derivatives of the current references are obtained by passing the signals through approximate differentiation filters

$$F(s) = \frac{ks}{\tau s + 1},$$

where $k = 1$ and $\tau = 0.0001$ s. The voltages of the capacitors C_1 and C_2 are initialized at $v_1(0) = 110$ V and $v_2(0) = 55$ V. The initial conditions of the DSER are taken as $i_1(0) = 3.24$ A and $i_2(0) = -6.12$ A.

To illustrate DSER, the time-varying energy-flow control gain $\alpha(t)$ shown in Figure 5 is implemented. As shown in Figure 5, in the time interval $[0, 0.32)$, the gain is chosen

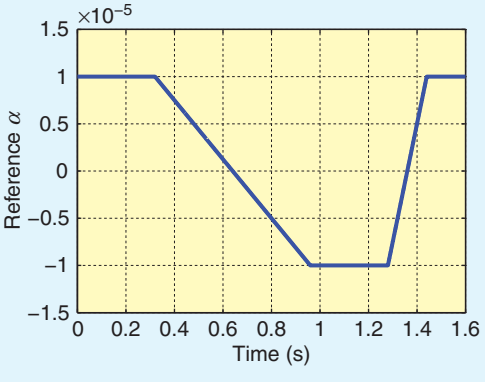

FIGURE 5 Time evolution of $\alpha(t)$, which controls the energy rate and direction. The variable $\alpha(t)$ can be constant or time varying, as shown in the plot. During the intervals [0, 0.32) s and (1.44, 1.6] s, $\alpha(t)$ is constant at the value 10^{-5}, while in the interval (0.96, 1.28) s, $\alpha(t)$ is constant at its lower value -10^{-5}. To test the dynamic response, two rates of change are imposed, namely, -31.25×10^{-5} s^{-1} and 125×10^{-5} s^{-1}.

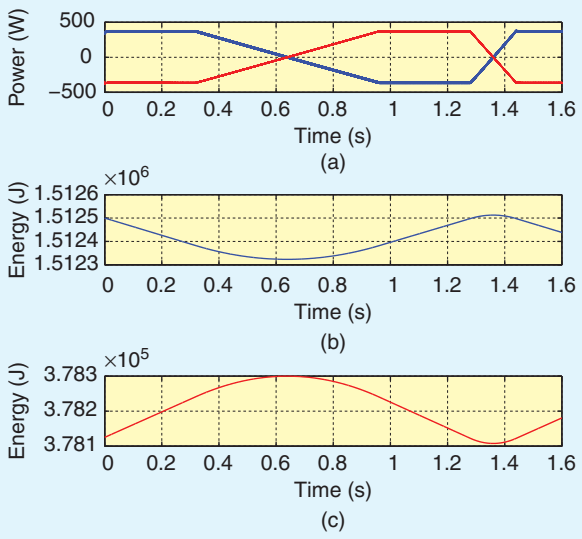

FIGURE 6 Time evolution of the power and energy variation in ports 1 and 2. (a) Power $\dot{H}_1(t)$ and $\dot{H}_2(t)$ in blue and red, respectively. One curve is the negative of the other, with a slight difference due to the ripple. Therefore, the energy supplied by one subsystem is stored by the other. Moreover, the waveform of the power delivered is proportional to $\alpha(t)$ with the same rates of change. (b) Energy evolution $H_1(t)$ in the capacitor C_1. (c) Energy evolution $H_2(t)$ in the capacitor C_2. At time 0 s the energy flows from C_1 to C_2, the flow starts to decrease at 0.32 s, and it is inverted at 0.64 s. Hence, after 0.64 s the energy flows from C_2 to C_1. At times 1.28 s and 1.44 s, where the waveforms cross zero, the total energy transfer is canceled. From time 1.44 s to 1.6 s the energy flows from C_1 to C_2 at the initial rate, and thus C_2 stores the energy delivered from C_1.

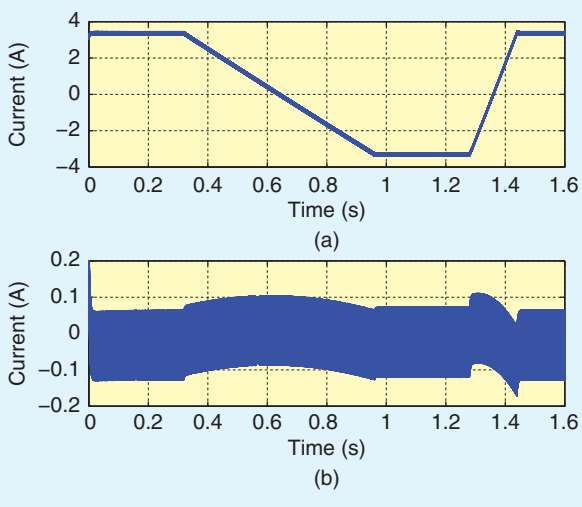

FIGURE 7 Time evolution of $i_1(t)$ and its error. (a) Current $i_1(t)$. Since the voltage in C_1 can be considered constant, the current $i_1(t)$ is proportional to $\alpha(t)$ with different units. In the intervals [0, 0.32) and (1.44, 1.6], i_1 reaches its maximum mean value of 3.65 A. The minimum mean value of −3.65 A is reached in the interval (0.96, 1.28). (b) Current error $\tilde{i}_1(t)$. The maximum mean value of the current error is 0.02 A, with a superimposed ripple of less than 5%. The ripple value can be reduced by increasing the switching frequency or by changing the inductance parameter, both according to the design criteria.

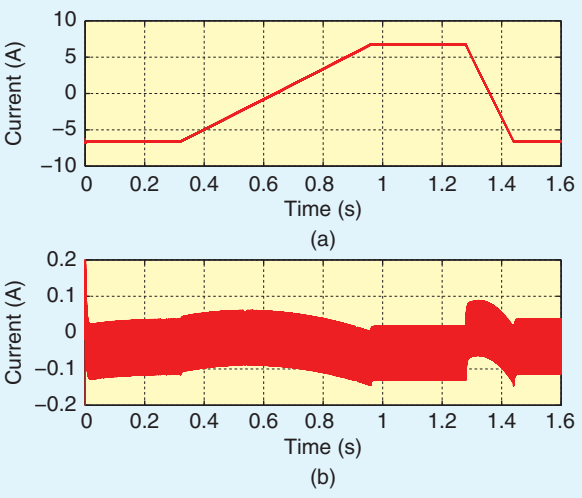

FIGURE 8 Time evolution of $i_2(t)$ and its error. (a) Current $i_2(t)$. The energy supplied by the capacitor C_1 has to be stored by the capacitor C_2, and consequently the current $i_2(t)$ has the same shape of $i_1(t)$ but with the opposite sign. During the intervals [0, 0.32) and (1.44, 1.6], i_2 reaches its minimum mean value of −6.35 A, and the maximum mean value is reached in the interval (0.96, 1.28). (b) Current error $\tilde{i}_2(t)$. The maximum current error is 0.025 A, which has a superimposed ripple of approximately 5%. The ripple can be improved by changing the design parameters.

to be constant and positive to rapidly transfer energy from Σ_1 to Σ_2. To deliver approximately 400 W, the gain is set to $\alpha(0) = 10^{-5}$. Then, in the time interval $[0.32, 0.96)$, the gain is slowly ramped down, crossing through zero, until it reaches $\alpha(0.96) = -10^{-5}$. Therefore, the transfer of energy from Σ_1 to Σ_2 slowly changes direction. In the interval $[0.96, 1.28)$ the gain is ramped up again, but with a faster rate, finally, keeping it positive and constant and returning to the initial scenario of transfer of energy from Σ_1 to Σ_2.

Figure 6 depicts the behavior of the instantaneous power and energy variation of Σ_1 and Σ_2, that is, $\dot{H}_1(t)$, $H_1(t)$ and $\dot{H}_2(t)$, $H_2(t)$, respectively. Figure 6 illustrates that energy transfer is achieved as desired, controlled by $\alpha(t)$ in both the direction and rate of change of the energy flow. As the energy is being transferred from one side to the other in the period of $[0, 0.64)$, the energy stored in the capacitor C_2 is initially increasing, while the energy stored in the capacitor C_1 is decreasing. The opposite situation takes place in the period $(0.64, 1.36)$. Both working conditions are shown in Figure 6.

The port currents as well as their references are shown in figures 7 and 8. Notice that the current ripple strongly depends on the switching frequency and the inductance L. Therefore, the 5% error could be improved in the DSER by increasing L or the commutation frequency. Figure 9 shows a zoom of the DSER capacitor voltage $v_C(t)$, which fluctuates around the reference 220 V. Fluctuations of less than 2%, even during severe changes of $\alpha(t)$ are observed, although in normal applications the tolerance is typically 5%.

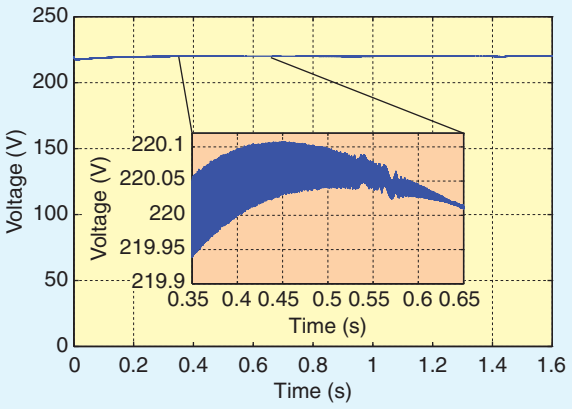

FIGURE 9 Time evolution of the voltage link capacitor $v_C(t)$. The nominal voltage of the link capacitor is 220 V, which is chosen according to the design criterion. Since the system is considered lossless and the energy is transferred completely from one capacitor to the other (C_1 to C_2 or vice versa), there is no stored energy in the link capacitor. Therefore, the nominal voltage remains, with less than 1% of variation, near 220 V during operation. The effect is shown by the magnified inset.

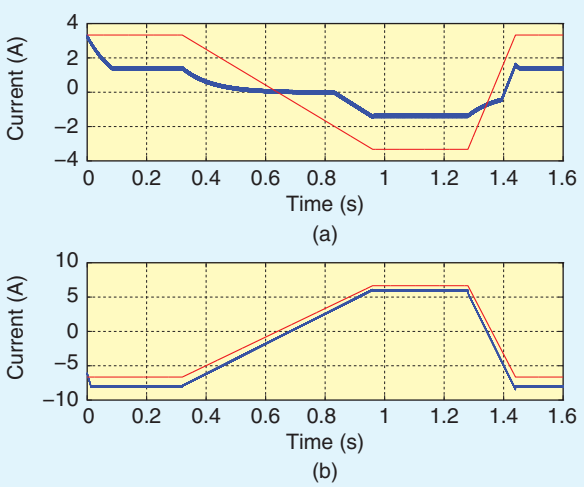

FIGURE 10 Time evolution of the currents and current references with $\gamma = 50$. (a) The current $i_1(t)$ in the left-side capacitor C_1 and its reference $i^*_1(t)$ are shown in blue and red, respectively. (b) Current $i_2(t)$ in the right-side capacitor C_2 and its reference $i^*_2(t)$ are shown in blue and red, respectively. In both waveforms (a) and (b), the displacement between the current reference and the load current can be noticed. Not only is the speed of convergence reduced but also the current remains away from its reference in steady state.

Although theoretically stability is ensured for all values of γ, the effect of the controller gain γ on the performance of the DSER is also studied by simulations. The same simulation is carried out for a smaller value of γ, namely, $\gamma = 50$. Figure 10 shows that, as expected from (18), the current tracking is significantly degraded. Consequently, the overall behavior of the DSER is also unsatisfactory, as shown in Figure 11.

CONCLUSIONS

A device to dynamically transfer energy between electrical multiports—the DSER—is presented and developed using standard switched power electronic devices. One of the central features of the DSER is the ability to control the direction and magnitude of the energy flow by changing only the parameter $\alpha(t)$, which comes directly from power port considerations. The importance of directly controlling the energy flow in microgrids is due to the ability to monitor the stocks as well as the consumption of energy in the various storage and source devices of the system. In an application of energy transfer involving batteries, for example, it is essential to be aware of the energy level of the batteries before making decisions about the appropriate energy control policy.

The performance of a dual-port DSER for a dc-to-dc application is verified by simulations. These simulations are carried out by applying a feedback linearization control law to the back-to-back dc/dc converter, which implements the DSER. The dc-to-dc transfer is of special interest due to its application to interconnected systems fed by proton exchange membrane fuel cells. Experimental facilities are available [10] to continue with this long-term project.

The potential applications of the DSER go beyond dc-to-dc configurations. Alternative topologies are available for handling ac-to-dc or ac-to-ac transfers. Furthermore, in this article we consider the interconnection of voltage sources, but in reality the energy in each port could be provided by current sources and a voltage-tracking system. These topologies, together with various control laws, are currently under study.

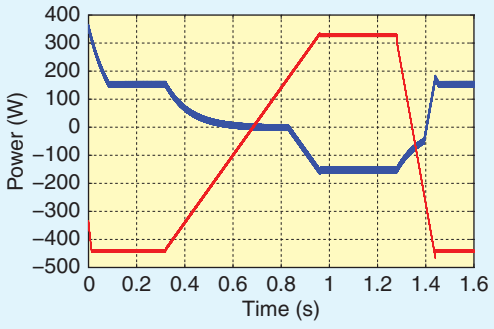

FIGURE 11 Time evolution of the system power with $\gamma = 50$. The power $\dot{H}_1(t)$ in the left-side port is in blue, while the power $\dot{H}_2(t)$ in the right-side port is in red. Since the shape of $\alpha(t)$ is not followed by the power profile of both capacitors, the complete performance of the interconnected system is deficient. The addition of delivered and demanded power is nonzero, and thus the remaining energy flows into the system. This energy difference interferes with the correct operation of the system by causing variations in the link-capacitor voltage $v_C(t)$. It is therefore necessary to account for the sensitivity of the static dc/dc power converter.

The goal of this article is to show that the DSER can be implemented by using standard power electronic converter topologies.

ACKNOWLEDGMENTS

The work of R. Griñó and S. Malo has been partially supported by the Spanish Research Project DPI 2007-62582. Antonio Sánchez-Squella would like to acknowledge Digiteo project 2007-13D and CONICYT–Embassy of France in Chile for their financial support.

AUTHOR INFORMATION

Antonio Sánchez-Squella obtained the B.Sc. in electrical engineering from the University of Concepción, Chile, in 2001. He received the M.Sc. in 2007 from Univeristè Paris-Sud 11, France, where he is currently working toward the Ph.D. From 2001 to 2006 he worked for the Industrial Support Company, Santiago, Chile, as a project engineer developing technological solutions for the copper mining industries in South America. His research interests are in nonlinear control and their application to energy management in electrical systems.

Romeo Ortega (ortega@lss.supelec.fr) obtained the B.Sc. in electrical and mechanical engineering from the National University of Mexico, the master of engineering from Polytechnical Institute of Leningrad, USSR, and the Docteur D'Etat from the Politechnical Institute of Grenoble, France, in 1974, 1978, and 1984, respectively. In 1984, he joined the National University of Mexico, where he worked until 1989. He was a visiting professor at the University of Illinois in 1987–1988 and at McGill University in 1991–1992, and he was a fellow of the Japan Society for Promotion of Science in 1990–1991. He is currently a CNRS researcher in the Laboratoire de Signaux et Systèmes (SUPELEC) in Paris. His research interests are in nonlinear and adaptive control and their applications. He is a Fellow of IEEE and an editor of several journals. He can be contacted at Laboratoire des Signaux et Systmes, SUPELEC, Plateau de Moulon, 91192 Gif-sur-Yvette, France.

Robert Griñó received the M.Sc. in electrical engineering and the Ph.D. in automatic control from the Universitat Politècnica de Catalunya (UPC), Barcelona, Spain, in 1989 and 1997, respectively. From 1990 and 1991, he was a research assistant at the Instituto de Cibernética, UPC. From 1992 to 1998, he was an assistant professor with the Systems Engineering and Automatic Control Department and the Institute of Industrial and Control Engineering, UPC, where he has been an associate professor since 1998. His research interests include digital control, nonlinear control, and control of power electronics converters. He is an affiliate member of the International Federation of Automatic Control (IFAC) and a member of the Comité Español de Automática (CEA)-IFAC. He is a Member of the IEEE.

Shane Malo received the B.Sc. in electronics engineering from the Universidad Francisco Marroquín (UFM), Guatemala City, Guatemala in 2001. In 2003 he joined the Institut d'Organització i Control de Sistemes Industrials at the Universitat Politècnica de Catalunya, in Barcelona, Spain, where he worked on the control of power electronics converters, obtaining the DEA in 2006, the M.Sc. in 2008, and the Ph.D. in 2009. From 2000 to 2002 he worked for Nortel Networks Corporation as a systems applications engineer in the deployment and analysis of TDMA and CDMA wireless access systems in Latin America. He is now with Ingeteam Technology S.A. working on power converters for high power applications. His research interests include power electronics, control of power converters, modeling of power converters, and alternative energy systems.

REFERENCES

[1] V. Duindam and S. Stramigioli, "Port-based asymptotic curve tracking for mechanical systems," *Eur. J. Control*, vol. 10, no. 5, pp. 411–420, Dec. 2004.

[2] V. Duindam, A. Macchelli, S. Stramigioli and H. Bruyninckx, *Geoplex–Consortium, Modeling and Control of Complex Physical Systems: The Port Hamiltonian Approach*. New York: Springer-Verlag, 2009.

[3] R. Ortega, A. Loria, P. J. Nicklasson, and H. Sira-Ramirez, *Passivity-Based Control of Euler–Lagrange Systems*. New York: Springer-Verlag, 1998.

[4] M. Hernandez-Gomez, R. Ortega, F. Lamnabhi-Lagarrigue, and G. Escobar, "Adaptive PI stabilization of switched power converters," *IEEE Trans. Control Syst. Technol.*, vol. 18, no. 3, pp. 688–698, 2010.

[5] R. Erickson and D. Maksimovic, *Fundamentals of Power Electronics*. New York: Kluwer, 2004.

[6] S. Malo and R. Griñó, "Design and construction of an electric energy conditioning system for a PEM type fuel cell," in *Proc. 33rd Annu. Conf. IEEE Industrial Electronics Society (IECON'07)*, Taipei, Taiwan, Nov. 2007, pp. 1633–1638.

[7] P. Thounthong, S. Raël, and B. Davat, "Utilizing fuel cell and supercapacitors for automotive hybrid electrical system," in *Proc. 20th Annu. IEEE Applied Power Electronics Conf. Exposition (APEC'05)*, Austin, Texas, USA, Mar. 2005, pp. 90–96.

[8] W. Choi, J. W. Howze, and P. Enjeti, "Fuel-cell powered uninterruptible power supply systems: Design considerations," *J. Power Sources*, vol. 157, pp. 311–317, June 2006.

[9] M. E. Schenck, J. Lai, and K. Stanton, "Fuel cell and power conditioning system interactions," in *Proc. 20th Annu. IEEE Applied Power Electronics Conf. Exposition (APEC'05)*, Austin, Texas, USA, Mar. 2005, pp. 114–120.

[10] R. Talj, D. Hissel, R. Ortega, M. Becherif, and M. Hilairet, "Experimental validation of a PEM fuel cell reduced order model and a moto-compressor higher order sliding mode control," *IEEE Trans. Ind. Electron.*, vol. 57, no. 6, pp. 1906–1913, 2010.